# On the interply friction of different generations of carbon/epoxy prepreg systems

Ylva R Larberg, Malin Åkermo*

Royal Institute of Technology, KTH, Dept. of Vehicle and Aeronautical Engineering, Teknikringen 8, SE-100 44 Stockholm, Sweden

*Corresponding author Tel.: +46 70 3206445, fax: +46 8 207865. E-mail address: akermo@kth.se (M. Åkermo).

## Abstract

Using pre-stacked material that is formed as a first step in the manufacturing process offers reduced process cycle time for production of complex structural components. The forming is achieved by forcing layers to deform by e.g. intraply deformation and interply slippage, where the latter is the scope of this study. The prepreg-prepreg friction is experimentally determined for four unidirectional carbon/epoxy prepreg systems. The materials differ considering volume fraction of fibres, fibre stiffness and phase of thermoplastic toughener (solved or particles). The study shows large individual differences between the tested materials, where the material systems with particle tougheners seem to obey a boundary lubrication friction, while the other materials show hydrodynamically dominated friction. A large difference between the high and low friction materials, almost a factor of 10, correlates to trends seen in the herein performed surface roughness measurements. Vacuum as well as autoclave consolidated materials are tested.

Keywords: A: Prepreg, Carbon fibre D: Forming, Surface analysis

# 1 Introduction

Increasing use of composite materials in commercial airliner applications creates a demand for higher efficiency and reduced labour and process cycle times, compared to the more traditional manual processes developed for small series aeroplanes. Using prepreg materials, the focus is on the lay-up process in order to avoid tedious manual steps and inter-mediate debulking. The automatic tape laying (ATL) machine as well as fibre placement have opened up for more efficient lay-up; however, since fibre placement still being a rather slow process and ATL put restrictions on the component geometries there is still a need for improvements. One alternative way to shorten the process cycle time of complex shaped structures is to perform efficient flat pre-stacking and then allowing the sheet to be formed prior to (or as a first step in) the curing process.

Forming a stack of prepreg requires that the material deforms according to the desired shape in a predictable way, without causing wrinkles or other faults. This is done by forcing the different layers to deform by intraply deformation (within the prepreg ply) and interply deformation (in-between the prepreg plies); both in the plane and due to bending of the fibres out of the plane. While previous studies [1,2] have shown large differences in the in-plane deformation behaviour in general (between different generations of prepreg materials), this paper focuses only on the in-plane interply deformation, or more exactly the resistance to interply deformation, by measuring the friction in-between separate prepreg plies.

The friction between the two sliding prepreg surfaces of non-cured composite prepreg materials has previously been reported to influence the quality of the formed composite component by causing residual stresses and shape distortions[3,4,5], core crushing during autoclave moulding of honeycomb sandwich components [6] and wrinkles due to resistance of forming. Other examples effecting the quality of the final component are prepreg

not properly laid up [3], slippage in corner areas and the different thermal expansion coefficients of the material and the tool [4,5]. During forming experiments, it has been shown that the microscopic thermoplastic particles used as tougheners (craze stoppers) greatly influence the degree of sliding within and between thermoset prepreg layers [1]. However, also process settings such as sliding rate, i.e. matrix shear rate, and matrix temperature has experimentally been shown to significantly influence the interply friction coefficient [2]. Several studies, e.g. [3,4], have concluded that friction initially drops as temperature increases. However, while the friction towards a metal tool continues to decrease at even higher temperatures, although still well below the resin curing temperature, the prepreg-prepreg friction reaches a minimum whereafter it increases again. Fibre intermingling is suggested as one reasonable explanation. Since it requires higher forces to shear a fluid at higher rate, frictional resistance has consequently been shown to increase with increasing sliding rate [7,8].

Comparing results from different studies, the influence of the normal force on the friction coefficient appears to follow the same trend for prepregs [6,7] as for dry, non-woven material (as e.g. polyester reinforcement [8]): At pressures in the magnitude of 0.1MPa, the friction coefficient is reported to decrease with increasing applied load. Further, the friction coefficient of dry, non-woven material is observed to decrease with increasing surface weight. The latter was explained by a more stable structure where less compaction was possible.

Most thermoplastic prepreg materials are often considered as having interply friction governed by the fluid matrix film in-between the prepreg plies, often referred to as hydrodynamic friction behaviour [9,10]. For these materials the prepreg-tool friction, as well as the interply prepreg friction, is fairly well understood and there are modelling tools available for predicting the friction load as function of material data or by parameter fit to experimental data.

This work aims to characterise the interply friction for four different non-bleeding, thermoset prepreg materials, for which initial tests in the workshop have indicated a more complex behaviour than purely hydrodynamic. In an earlier study [2] it was seen that although having seemingly similar characteristics (i.e. comparable type of fibres, matrix, fibre volume fraction, etc), the materials have shown significantly different interply friction. Two of the materials, of different prepreg generations, are therefore studied more thoroughly with the aim to determine governing mechanism controlling their interply friction. Both vacuum consolidated and autoclave consolidated samples are studied in order to see differences in frictional resistance coupled to degree of impregnation and fibre bed compaction achieved by consolidation. The study finally aims to relate the prepreg surface roughness to the interply prepreg friction.

## 2 Background

Friction between two surfaces in contact may be purely hydrodynamic, as when the two surfaces in relative motion are completely separated by a fluid lubricating film. In this case the friction may be predicted in terms of the traction forces acting on the film [11], neglecting the surface roughness effect on friction. For moderate loads hydrodynamic friction is independent of the normal load, but it is a function of matrix viscosity, film thickness and pulling rate according to

$$\tau = \frac{\eta}{d} v , \tag{1}$$

where $\tau$ is the shear stress, $\eta$ the matrix viscosity, $d$ the film thickness and $v$ the relative speed.

If no fluid separates the interface, the friction is governed by the force normal to the interface and generally described as Coulomb friction, i.e.

$$F = \mu N, \tag{2}$$

where $\mu$ is the friction coefficient and $N$ the normal force. However, for many types of surfaces, the film thickness is of the same order of magnitude, or less than, the combined roughness amplitude of the surfaces. In this case there will be areas with asperity contacts and areas with lubricating film contact. If the asperities in contact are separated by a thin film of molecular thickness this is referred to as boundary lubrication. The coexistence of two lubrication modes, hydrodynamic and boundary lubrication, is referred to as the regime of mixed lubrication. The asperity contact area is determined from geometric features of the surface and its ability to deform during applied normal force [11,12]. In composite applications it is expected that surface roughness in combination with matrix distribution is important to the interply friction behaviour. Martin et al [6] report that interply friction is significantly higher for woven prepreg materials when the matrix is concentrated to resin rich pockets on the surface, compared to when the entire surface is covered by a thin matrix layer.

The translation between different types of friction is visualised by the Stribeck theory [11]; initially developed to explain various types of friction in relation to the sliding rate, lubricant viscosity and bearing pressure in tribology. The Stribeck curve shows the Coulomb friction coefficient as function of the Hersey number given as:

$$H = \frac{\eta \nu}{p}, \tag{3}$$

where $\eta$ is the (dynamic) viscosity of the matrix, $\nu$ is the velocity at the contact surface and $p$ is the applied pressure. The example curve in Fig. 1 illustrates three different areas according to the type of friction taking place. The first region is governed by dry boundary lubrication similar to the Coulomb friction. The second part is a mixed mode friction, which

gradually translates into the third hydrodynamic region with increasing thickness of the lubrication layer. The friction coefficient in the hydrodynamic region thereafter increases with the thickness of lubricating layer. Please note that in Fig. 1 the normal force is used to calculate the Hersey number instead of the pressure, as in Eq. 3, wherefore the dimension differs. The Stribeck theory is verified by e.g. Ersoy et al [3] performing friction test under constant pulling rate, but changing temperature, for carbon/epoxy prepreg AS4/8552(i.e. similar to the one used in the present study). However, it is noted that with increasing temperature, the viscosity becomes too low to enable building up a sufficiently thick film to separate the sliding faces, wherefore the friction increases prior to curing initiation. Also in [7] the Stribeck curve is used to model interply friction. The Stribeck theory provides a mean to determine governing friction mechanisms at different process conditions by mapping the friction at different Hersey numbers.

Forming of multi-layered composites will result in different relative fibre orientations, which could have a significant impact on the frictional resistance. Martin et al [13] show that the friction will be higher when sliding along, 0°, the fibres compared to across, 90°, while Gorczyca-Cole et al [7] cannot see the effect of a lay-up change. In this study, the friction between layers oriented parallel to the pulling direction is investigated.

# 3 Experiments

## *3.1 Materials*

The different material systems included in this study are three aerospace graded systems and one experimental UD carbon/epoxy prepreg systems according to:

- HexPly® T700/M21 (referred to as T700/M21) from Hexel
- Cycom® HTS/977-2 (referred to as HTS/977-2) from Cytec
- HexPly® AS4/8552 (referred to as AS4/8552) from Hexel

- M21-IM (experimental material system based on a modified M21 and with a type of IM fibre, herein referred to as M21-IM) from Hexel

The first two materials are benchmark materials and more thoroughly tested. All systems are toughened by thermoplastics. In the case with the two different versions of M21, the tougheners are in form of particles initially mainly on the prepreg surfaces, while in HTS/977-2 and AS4/8552 the thermoplastics are in a liquid state. Fig. 2 shows the microstructure of HTS/977-2 and T700/M21 after curing and the virgin AS4/8552 material; where the lightest grey is the fibre, the darker grey is the matrix and the darkest grey in T700/M21 is the thermoplastic particles. As can be seen, AS4/8552 has dry regions in the centre. T700/M21 and HTS/977-2 have similar volume fraction of fibres ~57%, but the different distribution of matrix makes the local fibre volume fraction in T700/M21's fibre bed is higher than in HTS/977-2. The AS4/8552 prepreg used in this study is a company specific grade with a higher fibre volume fraction than the commercially available (i.e. >57%). The materials T700/M21 and M21-IM tested within this study have different distributions of thermoplastic particles. M21-IM shows a more even distribution on the surface, while T700/M21 also has particles within the fibre bed.

### *3.2 Sample preparation*

Two different versions of the materials were considered: virgin material and pre-consolidated material. The latter material was bagged onto a metal plate and consolidated in an autoclave with a cycle reaching 70ºC and 6 bar in order to reach the cured ply thickness, i.e. the requested degree of final consolidation. The purpose of this treatment is twofold; to obtain a surface similar to that during autoclave forming and to compact (smoothen) the fibre reinforcement. In order to ensure that the material remained at the cured ply thickness after

consolidation and prior to testing, the consolidated material was held under vacuum until tested.

### *3.3 Friction measurements*

The interlaminar friction between prepreg plies was measured using an in-house developed friction rig. The apparatus is shown in Fig. 3 and consists of one pneumatic cylinder and three plates holding the prepreg: one large (150 x 200 $mm^2$) fixed to the lower cross-head of the Instron 4505 testing machine and two smaller plates (100 x 90 $mm^2$) moving upwards as the test starts. The prepreg pieces were all clamped by a small metal plate tightened by screws, perpendicular to the fibre direction. To obtain isothermal conditions at elevated temperatures the apparatus was mounted inside a heating chamber, specially designed to fit the Instron 4505.

To start a test, sufficiently large pieces of prepreg were fixed onto the three plates under vacuum (-0.9 bar and 5 min), all fibres in the pulling direction. Other relative fibre orientations may have a significant effect, but is not investigated within this study. The prepreg cover film was kept on in order to secure a clean surface. The plates were thereafter mounted onto the test rig, the cover film removed, the oven closed and heating initiated. When the set temperature was reached, the rig was closed activating the pneumatic cylinder by increasing the air pressure to a level providing the desired normal force.

The load and displacement is measured using the Instron load cell (in this case 5kN) and machine position, respectively. The friction coefficient, $\mu$, is thereafter calculated from Eq. 2. At least three samples were tested for each test configuration. Further information on how the friction coefficient is extracted from test data can be found in [14].

All test configurations can be seen in Table 1. Please note that the viscosities cited herein are taken from curves provided by the material suppliers. For the M21-IM material, no specific viscosity curve has been provided. Due to its name it is assumed to be similar to the

other T700/M21, which simplifies comparison. However, until proven this should be considered a rough estimation. The different temperatures were selected based on initial experiments at SAAB Aerostructures and with the aim to test the materials at temperatures where their matrix viscosities are similar. However, it should be noted that the matrix viscosity given include toughening particles for T700/M21. Since the volume fraction of particles at the prepreg surface is approximately 35%, it is expected that the actual matrix viscosity (without particles) is lower [15]. The crosshead rate was selected based on realistic forming rates during sheet forming (vacuum forming) of pre-stacked prepreg material, given a geometry where a relatively small part is doubled curved, i.e. a beam with varied width and height. The normal pressures were selected to be in the range of vacuum pressure during sheet forming.

### *3.4 Surface roughness measurements*

The surface roughness of the different samples were scanned using the OptiTopo method [16], developed by Innventia, Sweden. With this technique, two images of the same region of a sample are acquired, where the different images are illuminated in a low angle from opposite directions. The height map was thereafter calculated using a photometric stereo technique. Frequency analysis was applied on the height map to separate the small-, mid- and large scale variations and their relative contribution. From this analysis the most interesting spectrum is presented as an image. Four areas of 12x12mm$^2$ were measured for each test piece.

The advantage of this method compared to more traditional surface measuring devices is that it enables registering the topology of soft surfaces, which is difficult with techniques based on a travelling needle. Further, is seems to work without any problems with reflectance, which can be a problem for laser assisted surface roughness measuring devises.

Since OptiTopo measurements are preformed at room temperature, only remaining changes due to heat treatments can be registered.

The samples for the surface roughness measurements were all vacuum consolidated (-0.9 bar and 5 min) towards a plane steel plate to simulate the surfaces in the friction rig. For heat treatment, the surface films were removed and the plates heated up to the same temperature as used during friction testing. The plates were then removed from the oven and test samples cut from the cooled material.

# 4 Discussion of results

The results are presented considering first the measured friction coefficient for all virgin materials investigated with the aim to see the general trends, whereafter results from further studies on the benchmark materials are presented. The influence of autoclave consolidation on the interply friction and the influence of surface roughness are discussed considering all non-consolidated materials in the study.

Fig. 4 shows the friction coefficient as function of matrix viscosity for all virgin material systems investigated; however, recall that the viscosity of M21-IM is based on a rough estimation. Most notably is the large difference in friction between the different material systems tested: the friction coefficient for T700/M21 is roughly 10 times higher than for HTS/977-2 at the same viscosity. The friction coefficient for AS4/8552 is almost half that of T700/M21 at the lower viscosities; however, at higher viscosities it is in the same range. Further, M21-IM has a friction coefficient almost as low as HTS/977-2 for the considered viscosity, i.e. only 17% of the friction coefficient of the benchmark T700/M21.

Taking a closer look at each individual material it can be observed that the friction coefficient is generally higher at the lowest viscosities investigated compared to at slightly higher viscosities. This is in agreement with earlier investigations [6,7], where the fibre

entanglement and lack of load bearing capacity of the matrix was then suggested as possible reasons. There seems to be a vague minimum as the viscosity decreases to around 250 Pa·s.

As can be seen, at the higher viscosities investigated the friction coefficient increases with increasing viscosity. Theory gives that if the friction is purely hydrodynamic and if the matrix film thickness is constant at the higher viscosities, the friction is linearly dependent on the viscosity and approximately 5 times higher at 1000 Pa·s than at 200 Pa·s, see Eq. 1. As can be seen, this is not the case for any material tested: for the AS4/8552 material the increase in friction is 60%, instead of 300%, for the given span of viscosities while for T700/M21 the friction coefficient is seemingly constant and independent of matrix viscosity at viscosities higher than 250 Pa·s. While the former (AS4/8552) still largely depends on the matrix viscosity and thus have significant contributions from hydrodynamic friction, the latter (T700/M21) show a more Coulomb like friction behaviour at viscosities higher than 250 Pa·s.

Fig. 5 shows one characteristic load-deformation curve for each material system tested. As can be seen, the load increases rapidly and almost linearly with increasing deformation up to a maximum level whereafter the load–displacement curve changes and almost flattens out (not entirely for T700/M21). No curve shows typical stick-slip peak characteristic for dry Coulomb friction. The steadily increasing load at higher displacements is most pronounced for T700/M21, but similar weaker tendencies can also be seen for AS4/8552 and M21-IM (hard to see in this figure due to the scale). The reason for this is not fully understood. However, the friction is expected to increase as surface resin is worn away and the remaining surfaces become even rougher. No signs of resin build up in front of the sliding test rig can be detected. The non-linear character of the load response seen for some materials can have a significant effect on the forming, especially in cases where the degree of slippage is small; however, the phenomenon is not further investigated within this study.

Fig. 6 illustrates the influence of relative speed on the friction coefficient for the two benchmark materials HTS/977-2 and T700/M21. As can be seen, the two materials show different behaviour, where the friction coefficients for T700/M21 is stable within the test interval (differences are within experimental errors). For HTS/977-2, on the other hand, the friction coefficient increases with increasing relative speed. The friction at a relative speed of 1 mm/min is 2.75 times higher than at 0.1 mm/min. Eq. 1 predicts that for pure hydrodynamic behaviour the interply friction increases linearly with speed. Higher friction coefficients at higher velocities are in agreement with observations during tests on the deformability of multi-layer HTS/977-2 material [2], where rate dependent slide band width indicated increasing interply friction at higher deformation speeds. Also, the seemingly constant friction coefficient for T700/M21 at low velocities are in agreement with previous results on T700/M21 multilayer materials [2], where the slide bands are constant for different deformation rates within the test interval. The interply friction for T700/M21 is not rate dependent and therefore indicates boundary lubrication, see Fig.1.

The influence of normal force on the friction coefficients for the two benchmark materials is similar, see Fig. 7. In agreement with previous studies and experiments on fibrous materials [8], the friction coefficient initially decreases with increasing normal pressure. However, upon further increasing pressure, the friction coefficient remains stable, in accordance with the definition of boundary friction. This indicates that the initially rough and partly porous fibre material gives a higher friction coefficient, possibly due to spring back of fibres during heating up. The higher pressure will reduce the roughness and the friction coefficient decreases to a level where no further compaction is possible.

As exemplified in Fig. 8, the influence of pressure on the friction coefficient also depends on the matrix viscosity and for the HTS/977-2 material the sensitivity to pressure is larger at low viscosities than at the higher viscosities tested.

The findings considering the benchmark materials are further empathised considering the Stribeck curves, shown in Fig. 9. The measuring points for the HTS/977-2 material seem to adopt well with the translation from the mixed lubrication to the hydrodynamic region, while the measuring points for the T700/M21 material does not show a clear trend that can be easily traced back to the different regions of the Stribeck curve. For T700/M21 the values are either exactly in the friction minimum in the mixed lubrication zone or on the plateau in the boundary lubrication area where Coulomb friction dominates. Even though the latter seems a bit awkward considering the soft matrix and particle rich layer on the prepreg surface, see Fig. 2, all measurements presented earlier further support that this simple model enables describing the dominating trends for the T700/M21 material.

### *4.1 Influence of prepreg consolidation*

In Table 2 the influence of prepreg consolidation on friction coefficient is listed. As can be seen, for HTS/977-2 the consolidated material gives roughly 70% lower interply friction compared to the virgin material, while for all other materials the friction coefficient goes up. For T700/M21 and M21-IM this is expected since consolidation fuse the particles into the fibre bed, limiting their possibility to roll. Further, consolidation forces the matrix into the fibre bed possibly making the surface particles somewhat resin starved. As can be seen, the friction coefficient increases with 63% for M21-IM, but only 27% for the benchmark T700/M21 with fewer particles concentrated on the prepreg surface.

It was not expected to find such large increases in friction coefficient for the autoclave consolidated AS4/8552 material. Fig. 10a shows that for this material, the entire interply deformation behaviour changes due to consolidation: for autoclave consolidated material the load deformation curve indicate a more viscous deformation with a smoother transition reaching its maximum at much higher degree of deformation. For all other materials

the load-deformation curve shows the same characteristics for the consolidated material as for the vacuum-consolidated materials. This non-linearity could have a significant impact on the forming, but is not investigated further within this study. As can be seen in Fig. 10b, for AS4/8552 the difference in friction coefficient between autoclave consolidated and vacuum consolidated material decreases significantly as the viscosity decreases. The AS4/8552 material is tested at higher viscosities compared to the HTS/977-2 material and it is possible that upon further heating (i.e. reduction of matrix viscosity and fibre spring back) the friction coefficient for the AS4/8552 material would reduce further towards the level for the autoclave consolidated HTS/977-2 material. However, this needs to be further investigated in following studies.

### *4.2 The relation between surface roughness and friction coefficient*

All virgin materials in this experimental series are initially slightly compacted from the vacuum pressure used to fix the material towards the friction plates. Increasing the temperature (reducing the viscosity) may result in material spring back, which increases the surface roughness of the tested material compared to the room temperature material. In this study, the surface roughness is reported as the root mean square (RMS) value, the statistical measure of the magnitude of a varying quantity. The mean level of the surface is calculated along a thousand lines, all perpendicular to the fibre direction and the values presented as the measure of surface roughness is consequently the deviation from this mean level. The errorbars show the spread of the four areas within each tested specimen.

Fig. 11 shows the surface roughness of the virgin materials at room temperature and after heat treatment to different temperatures. As can be seen, as delivered, the surface roughness is significantly (~40%) higher for T700/M21 and AS4/8552 compared to HTS/977-2 and M21-IM, which is in good agreement with the major trends presented considering the friction coefficient of the different materials at corresponding viscosities; see Fig. 4. Heating the

material to 70°C, the roughness increases with almost 30%. Upon further heating to 85°C, the roughness of the two benchmark materials almost coincide. Fig. 8 shows that for HTS/977-2, the friction coefficient is 50% higher for the sample heat treated to 80°C compared to the sample heat treated to 70°C. The difference in surface roughness is 20%. As can be seen for T700/M21 the surface roughness is seemingly steady at temperatures above 70°C. That the friction coefficient is 20% higher at the lowest viscosity (85°C) compared to at higher viscosities can therefore not be explained from the surface roughness measurements only, but possibly depends on that the particles are more resin starved or that the low viscosity matrix does not carry load in the same way as at higher viscosities. Due to its composition, M21-IM is expected to follow a similar trend as T700/M21, while AS4/8552 is expected to appear more like the HTS/977-2 material. Fig. 12 shows the measured surface topologies of all materials after heat treatment to 70°C.

Normalising the friction coefficient with respect to matrix viscosity enables comparing values at different temperatures. Considering results from tests performed at the same normal pressure and pulling speed, the normalised friction coefficient shows a clear dependency on surface roughness for all materials tested, see Fig 13. In fact, also tests performed at different normal pressures would fit into the figure, showing up as a scatter around the baseline result. For T700/M21 this scatter is however very large. It is interesting that all materials seem to follow the same trend, although T700/M21 and M21-IM includes hard thermoplastic particles on the surface: As can be seen, the normalised friction seems initially linear with surface roughness, but since the surface roughness does not increase infinitely (it is limited by the fibre reinforcement texture), and the normalised friction coefficient increases at low viscosities (higher friction and lower viscosity), the curve develops to exponential form.

Considering the simplest equation for hydrodynamic friction, Eq. 1, it seems reasonable to normalise the friction coefficient with respect to both viscosity and pulling rate, concluding that there is a relation between increased RMS and decreased thickness of the surface matrix film. However, while this enables to better gather the results from the HTS/977-2 material around the line shown in Fig. 13, due to different governing mechanisms, the T700/M21 results deviates even more from the shown trend. Further tests are needed to further explore the validity of this curve.

The influence of autoclave consolidation on surface roughness was not investigated in this study due to limited amount of material.

To state which the ideal frictional properties are is difficult. It seems to differ depending on the deformation mechanism preferred, based on for example the relation between forming mechanisms, geometry of the tool and stacking sequence. A low friction often results in more slippage and less fibre rotation, which in extreme situations have resulted in areas with "washed away" layers. A material system with a higher friction may behave more predictable during forming, which could lead to a more robust forming process than with a low friction system.

# 5 Conclusions

The interply (prepreg-prepreg) friction coefficient for four different aerospace graded carbon/epoxy prepreg systems has been measured using a dedicated rig. The material differs considering volume fraction of fibres, fibre stiffness and the type of toughener. Two material systems with and without particles, were benchmark materials and more thoroughly studied. In addition to measurements on the virgin materials, a smaller number of tests have been

performed on materials pre-consolidated in an autoclave. The friction test measurements were complemented with surface roughness measurements.

The results show significant differences between the studied materials, which roughly are divided into two groups; one with high and the other with low friction coefficient. The high friction materials, i.e. the benchmark material with particles and the no-particle material with higher volume fraction of fibres, have roughly 10 times higher friction coefficient than the low friction material, i.e. the benchmark material without particles and the particle material with stiffer fibres. A similar trend is seen from the surface roughness measurements where the same two groups of materials show significantly different surface roughness. The RMS value differed with approximately 40% between the two groups.

All materials studied show higher interply friction at the highest measured temperatures (lowest viscosities) compared to at slightly lower temperatures. Further, the friction coefficients for both of the benchmark materials decrease with increasing normal pressure, this up to a certain level where the friction coefficient is stable. Both results indicate that fibre bed compaction influences the friction coefficient significantly.

The results show that the friction coefficient for the benchmark material with toughening particles seem to be fairly stable, which means independent of both matrix viscosity and relative interply deformation rate. For the no-particle benchmark material, on the other hand, the friction coefficient increases with both increasing viscosity and relative interply deformation rate. While the latter indicates hydrodynamic friction behaviour, the former seems to obey Coulomb type friction.

Pre-consolidation of the prepreg material seems to fuse the toughening particles into the fibre reinforcement at the same time as it becomes slightly resin starved, which significantly increases the interply friction coefficient. The influence on consolidation on the other two materials tested seems to be very material dependent.

Independently of material system, the friction coefficient of all material systems tested at similar conditions (normalised with respect to matrix viscosity) show an exponential dependency on prepreg surface roughness. The validity of this relation needs to be further investigated.

## Acknowledgements

The work financed by the Swedish National Aeronautical Research Program (NFFP) and the KTH Production Technology Platform XPRES. Thanks to Per Hallander and Mikael Peterson at Saab AB, and Hans Christiansson at Innventia for cooperation and support.

**REFERENCES**

1. Larberg YR, Åkermo M. In-plane properties of cross-plied unidirectional prepreg. In: Proceedings of ICCM-16 Conference, Kyoto, Japan, July, 2007.
2. Larberg YR, Åkermo M. On the deformability of different generations of cross-plied unidirectional prepreg. Submitted to Journal of Composite Materials, 2010.
3. Ersoy N, Potter K, Wisnom MR, Clegg MJ. An experimental method to study the frictional processes during composites manufacturing. Composites Part A, 2005; 36A: 1536–1544.
4. Ersoy N, Garstka T, Potter K, Wisnom MR, Porter D, Stringer G. Modelling of the spring-in phenomenon in curved parts made of a thermosetting composite. Composites Part A, 2010; 41: 410–418.
5. Arafath ARA, Vaziri R, Poursartip A. Closed-form solution for process-induced stresses and deformation of a composite part cured on a solid tool: Part I – Flat geometries. Composites Part A, 2008; 39: 1106–1117.

6. Martin CJ, Seferis JC, Wilhelm MA. Frictional resistance of thermoset prepregs and its influence on honeycomb composite processing. Composites Part A, 1996; 27A: 943–51.

7. Gorczyca-Cole JL, Sherwood JA, Chen J. A friction model for thermostamping comingled glass-polypropylene woven fabric. Composites Part A, 2007; 38: 393-406.

8. Kalebec NA, Babaarslan O. Effect of weight and applied force on the friction coefficient of the spunlace nonwoven fabrics. Fibers and Polymers 2010, 11(2): 277-284.

9. Thije RHW, Akkerman R. Finite Element Simulations of Laminated Composites Forming Processes, In: Proceedings of ESAFORM-13 Conference, Brescia, Italy, April, 2010.

10. Vanclooster K, Lomov SV, Verpoest I. Simulation of Multi-Layered Composites Forming. In: Proceedings of ESAFORM-13 Conference, Brescia, Italy, April, 2010.

11. Stachowiak GW, Batchelor AW. Engineering tribology, Butterwoth-Heinemann, 2000.

12. Wang W-Z, Wang S, Shi F, Wang Y-C, Chen H-B, Wang H, Hu Y-Z. Simulations and measurements of sliding friction between rough surfaces in point contacts: From EHL to boundary lubrication. Journal of Tribology, 2007, July (129): 495-501.

13. Murtagh AM, Lennon JJ, Mallon PJ. Surface friction effects related to pressforming of continuous fibre thermoplastic composites. Composites Manufacturing, 1995, 6: 169-175.

14. Larberg YR, Åkermo M. On the interply friction of different generations of unidirectional prepreg materials. In: Proceedings of ECCM-13, Stockholm, Sweden, June, 2008.

15. Laun HM, Bung R, Hess S, Loose W, Hess O, Hahn K, Hädidicke E, Hingmann R, Schmidt F, Lindner P. Rheological and small angle neutron scattering investigation of sheer-induced particle structures of concentrated polymer dispersions submitted to plane Poiseuille and Couette flow. Journal of Rheology, 1992, 36(4): 743-878.

16. OptiTopo method, http://www.innventia.com/templates/STFIPage_7384.aspx.

Table 1. Test matrix for prepreg-prepreg friction.

| Material | Temperature [°C] | Pressure [kPa] | Load speed [mm/min] | Viscosity [Pa·s] |
|---|---|---|---|---|
| 977-2 | 70 | 53/80/120 | 0.1 | 120 |
| | 70 | 53 | 0.05/0.1/1 | 120 |
| | 80 | 80/120 | 0.1 | 50 |
| | 80 | 53 | 1 | 50 |
| | 60 | 80 | 0.1 | 400 |
| 977-2, consolidated | 80 | 80 | 0.1 | 50 |
| M21 | 60 | 80 | 0.1 | 1500 |
| | 70 | 80 | 0.1 | 300 |
| | 85 | 53/80/120 | 0.1 | 90 |
| | 85 | 80 | 0.05/0.1/1 | 90 |
| M21, consolidated | 70 | 80 | 0.1 | 300 |
| M21-IM | 70 | 80 | 0.1 | *300** |
| M21-IM, consolidated | 70 | 80 | 0.1 | *300** |
| 8552 | 45 | 80 | 0.1 | 1000 |
| | 58 | 80 | 0.1 | 400 |
| | 70 | 80 | 0.1 | 180 |
| 8552, consolidated | 45 | 80 | 0.1 | 1000 |
| | 70 | 80 | 0.1 | 400 |

* Approximation based on the values given for M21

Table 2. Friction coefficient for autoclave consolidated compared to vacuum compacted taken at a displacement of 1 mm.

| Material | Temperature [°C] | Friction coefficient, virgin [N/N] | Friction coefficient, autoclave [N/N] | Difference in % |
|---|---|---|---|---|
| M21 | 70 | 0.22 ± 0.030 | 0.28 ± 0.016 | +27 |
| M21-IM | 70 | 0.019 ± 0.0026 | 0.031 ± 0.0045 | +63 |
| 977-2 | 80 | 0.031 ± 0.0075 | 0.0088 ± 0.0012 | -72 |
| 8552 | 45 | 0.12 ± 0.039 | 0.64 ± 0.0047 | +433 |
| | 70 | 0.081 ± 0.026 | 0.20 ± 0.026 | +147 |

All figures except 1 and 12 are meant to be in colour on the web.

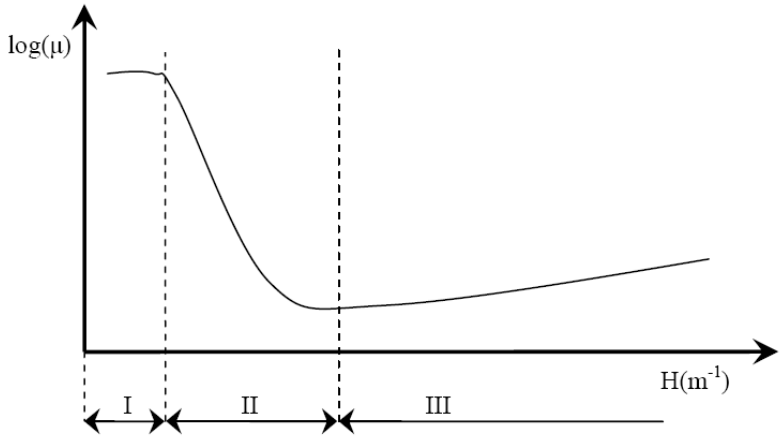


Fig. 1. Example of a Stribeck curve; Area I: boundary lubrication; II: mixed lubrication; III: hydrodynamic lubrication [7].

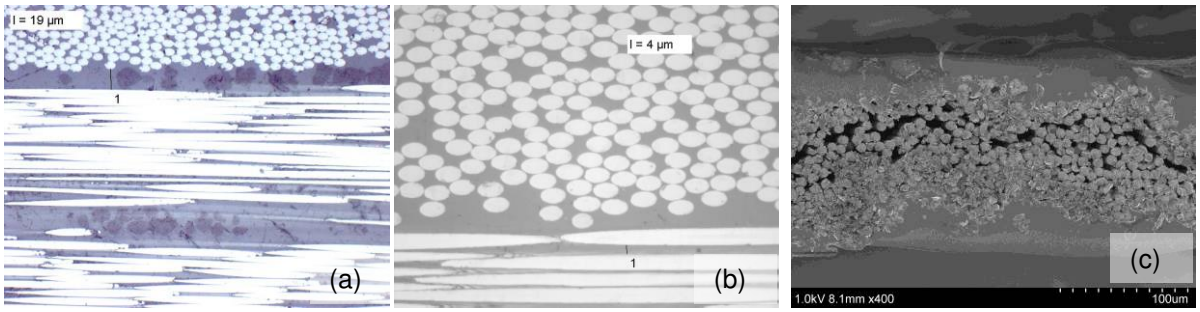


Fig. 2. Microstructure of prepreg laminates a) consolidated and cured T700/M21 (x500) b) consolidated and cured HTS/977-2 (x1000) (Courtesy of Per Hallander, Saab AB, Linköping, Sweden), c) unconsolidated and uncured AS4/8552 (x400) (note the different scales).

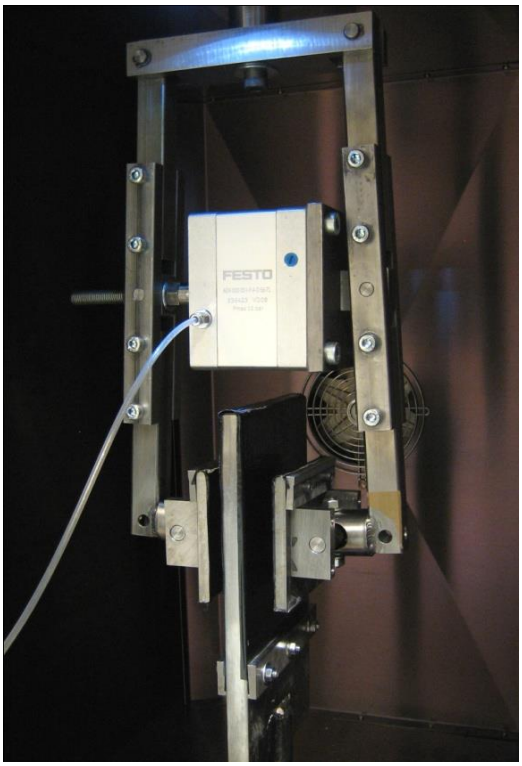


Fig. 3. Friction rig for measurement of interply friction.

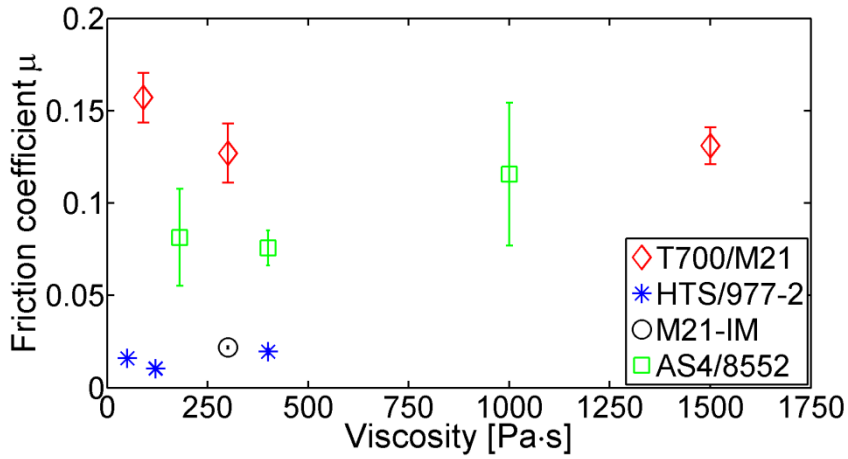


Fig. 4. Coefficient of interlaminar friction at different viscosities.

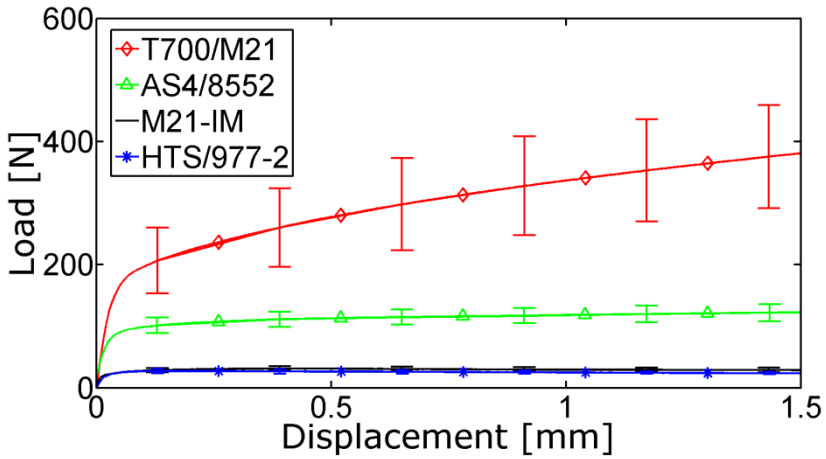


Fig. 5. Load curves from interlaminar tests for all four materials at approximately the same viscosity; 300-400Pa·s.

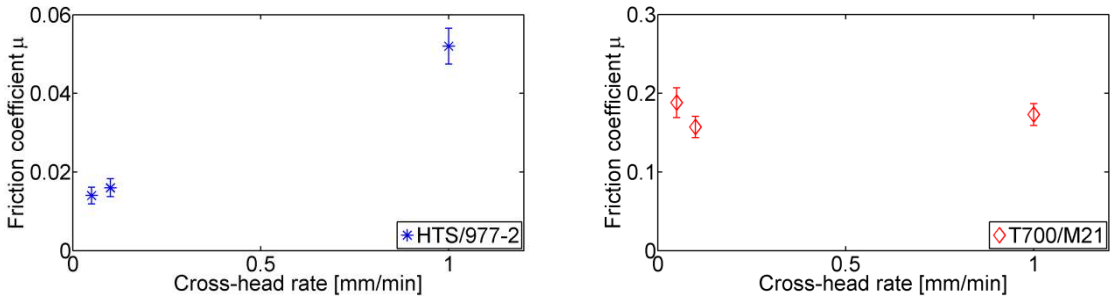


(a) (b)

Fig. 6. Friction coefficient as function of relative speed (cross-head rate): a) HTS/977-2 at an applied pressure of 53kPa, 70°C and b) T700/M21 at an applied pressure of 80kPa, 85°C.

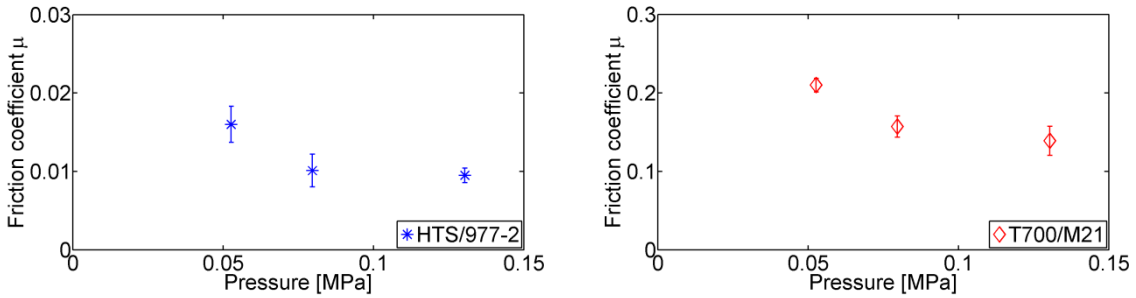


(a) (b)

Fig. 7. Friction coefficient as function of applied pressure at relative speed 0.1mm/min a) HTS/977-2 70°C and b) T700/M21 is tested at 85°C.

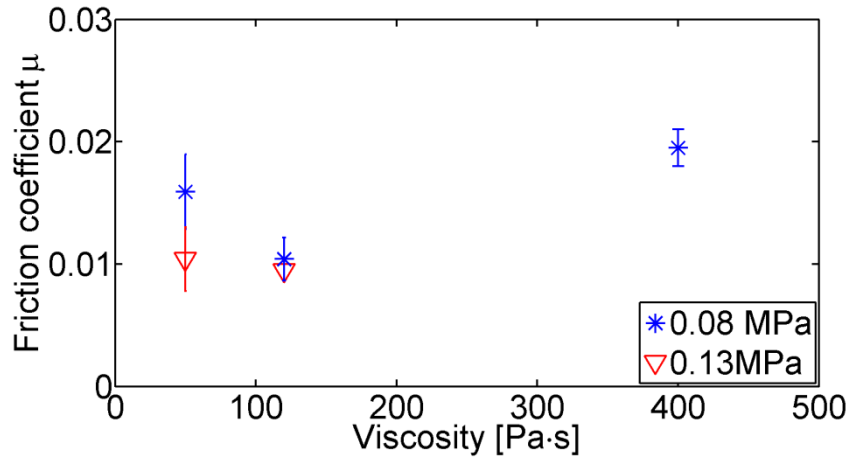


Fig. 8. HTS/977-2 tested at 0.1mm/min, results from two different temperatures and two applied pressures.

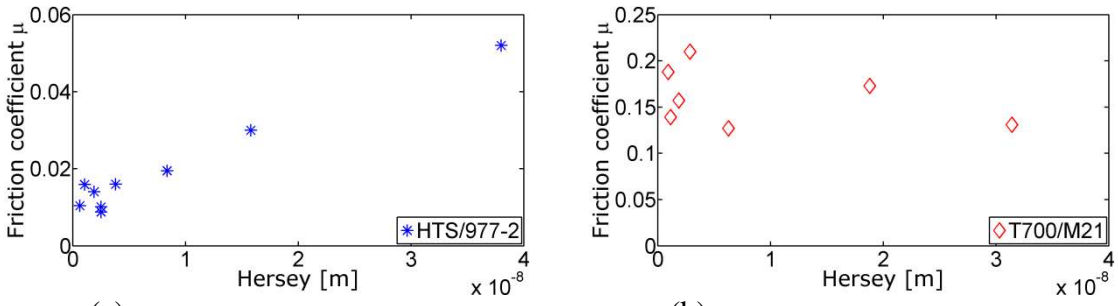


(a) (b)

Fig. 9. Stribeck plots for a) HTS/977-2 and b) T700/M21. Note the different scales!

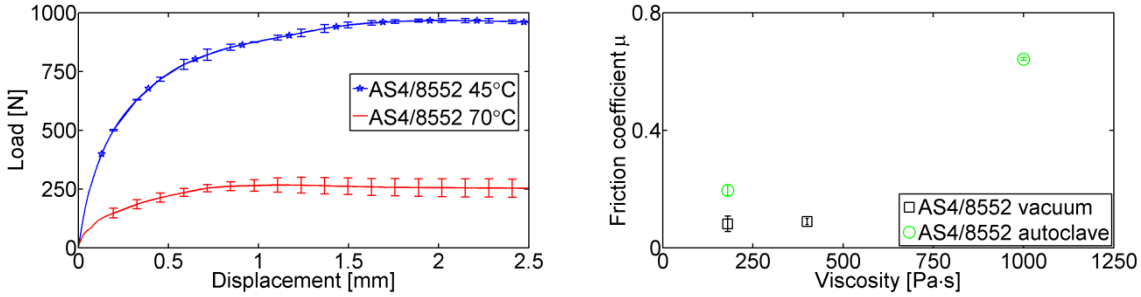


(a) (b)

Fig. 10. a) Load-displacement of autoclave consolidated AS4/8552 and b) friction coefficient for AS4/8552 at 0.1 mm/min at 80kPa (values taken at 1 mm) to the right.

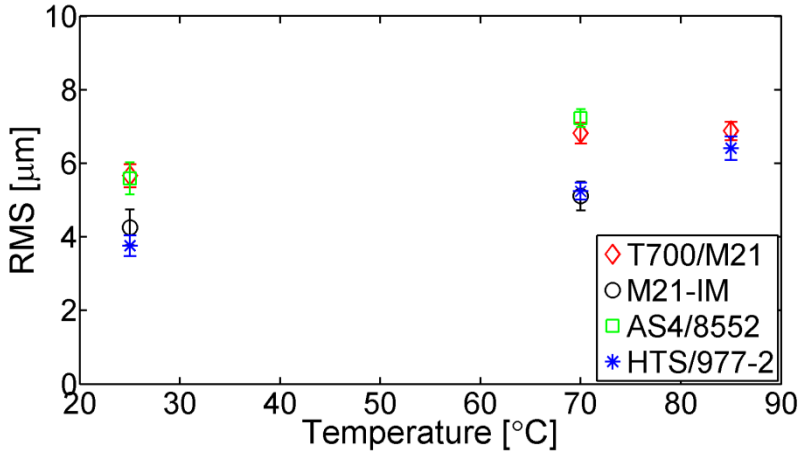

Fig. 11. Prepreg surface roughness versus heat treatment temperature

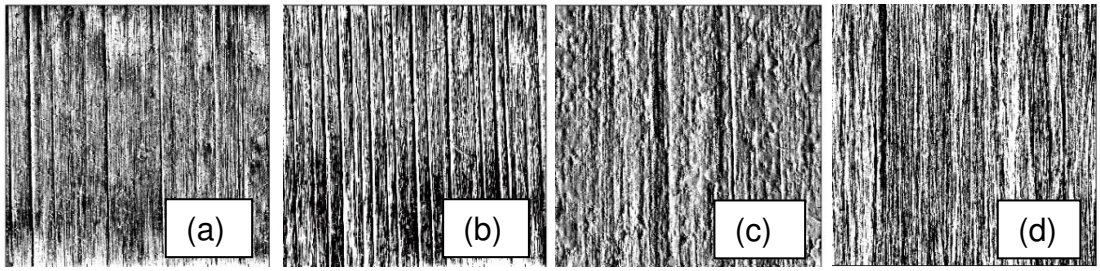

Figure 12. Surface topology after heat treatment up to 70°C for a) HTS/977-2, b) AS4/8552, c) M21-IM and d) T700/M21, each area 12x12mm$^2$.

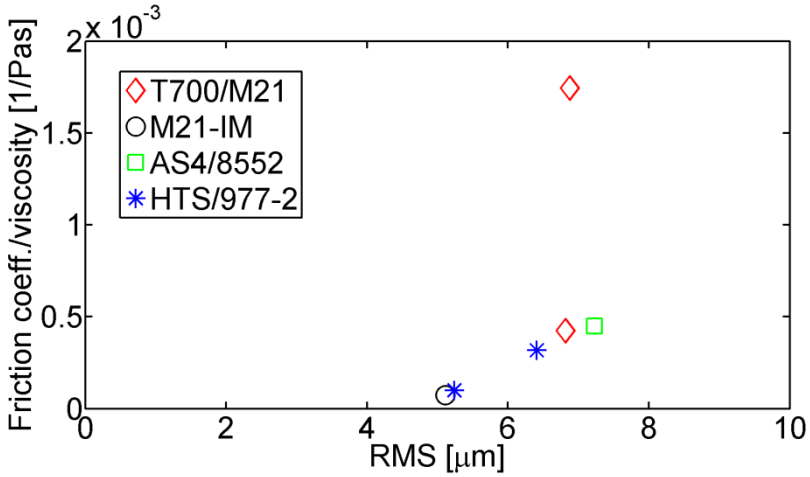

Fig. 13. Friction coefficient normalised with viscosity as function of prepreg surface roughness.